energies

MDPI

Article

The Influence of Injector Nozzle Diameter on High-Density and Lean Mixture Combustion in Heavy-Duty Diesel Engines

Yize Liu * and Wanhua Su

State Key Laboratory of Engines, Tianjin University, Tianjin 300072, China
* Correspondence: liuyize@tju.edu.cn

Abstract: In order to improve the fuel economy of heavy-duty diesel engines under high-load conditions, based on the combustion pathway model, it is proposed that the proportion of lean mixture with $0 < \Phi < 1$ is the most important spray characteristic affecting the overall diesel combustion process. Answering the question of how to increase the proportion of lean mixture inside the spray is the key to achieving the efficient and clean combustion of diesel engines. This paper investigated the mechanism of injector nozzle diameter on the in-cylinder air–fuel mixture and combustion process based on a high-density and lean mixture characteristic combustion strategy. The experimental results show that with an increase in nozzle diameter, the peak pressure and instantaneous heat release rate significantly increase, the combustion duration is shortened by about 20%, and the heat release becomes more concentrated. At 1200 rpm and IMEPg~2.3 MPa conditions, the indicated thermal efficiency increases by 1.3%, reaching a maximum of 51.5%. The numerical simulation results show that with the increase in nozzle diameter from 0.169 mm to 0.218 mm, the spray ejection momentum per unit time increases by 30%, the momentum transferred to the air by the spray increases, the oxygen transport process becomes more intense, and the air entrainment mass during the spray free development stage increases by 42%. The proportion of lean mixture inside the spray throughout the entire spray development process increases, resulting in an increase in the heat release rate of the lean mixture, making the overall combustion more intense and concentrated.

Keywords: heavy-duty diesel engine; injector nozzle diameter; lean mixture; spray characteristic; air entrainment; fuel–air mixing; thermal efficiency

Citation: Liu, Y.; Su, W. The Influence of Injector Nozzle Diameter on High-Density and Lean Mixture Combustion in Heavy-Duty Diesel Engines. *Energies* **2024**, *17*, 2549. https://doi.org/10.3390/en17112549

Academic Editor: Dimitrios C. Rakopoulos

Received: 24 April 2024
Revised: 17 May 2024
Accepted: 22 May 2024
Published: 24 May 2024

1. Introduction

In order to address the environmental issues brought about by global climate change, the Paris Agreement aims to reduce greenhouse gas emissions to near zero by the end of this century [1]. Road transport accounts for 72.06% of greenhouse gas emissions from the transport sector as a whole, and the diesel engine is still the most widely used means of road transportation [2,3]. The intensification of energy consumption and the urgent need for environmental protection have prompted the upgrading of traditional diesel engine technology to meet the requirements of efficient and clean combustion.

In order to further improve the thermal efficiency of diesel engines, extensive research has been carried out on combustion modes and various innovations have been made. In terms of combustion theory, the pursuit of in-cylinder homogeneous charge combustion became a key research direction for internal combustion engines following the proposal of the homogeneous charge compression ignition combustion mode [4]. However, this combustion mode still had some difficulties, such as high pressure rise rate and limited operating load [5]. Under heavy-load conditions, diesel engines predominantly use diffusion combustion. The large cycle fuel injection mass and slow heat release rate limit the improvement of thermal efficiency.

Researchers have made significant progress in the development of high mixing rate combustion technology for diesel engines [6,7]. The parameters of the fuel injection system

determine the initial fuel injection momentum and the subsequent fragmentation and entrainment process. Zhai [8] et al. investigated the effect of injector nozzle diameter on injection characteristics under different injection pressure conditions. As the injection pressure increases and the injector nozzle diameter decreases, the time for the liquid length to reach a stable stage is shortened, and strong oxidation reactions are simultaneously distributed in both the upstream and downstream regions of the flame. Compared to using a micro-hole diameter (D = 0.07 mm, Pinj = 100 MPa), increasing the injection pressure to 300 MPa (D = 0.133 mm, Pinj = 300 MPa) can more effectively reduce the soot produced per unit of fuel mass and improve the thermal efficiency of diesel engines. The increase in fuel injection pressure enhances the speed of radial air entrainment at the initial stage of fuel injection, which increases the spray angle and significantly improves the fuel–air mixing rate [9,10]. Shi [11] et al. studied the effect of injection pressure on the combustion characteristics of diesel engine low-temperature wall-impinging ignition, finding that increasing the injection pressure is beneficial for optimizing high-temperature combustion but may lead to unstable low-temperature ignition. With an increase in the injection pressure from 40 MPa to 100 MPa, the ignition delay at 840 K ambient temperature initially shortened and then prolonged, with the combustion condition being best at 80 MPa. Reducing the fuel injection mass is detrimental to low-temperature ignition, as the ignition transitions from stable to unstable, and then to misfire, as the injection mass decreases from 35–50 mg to 20–30 mg, and further to 15 mg. Comprehensive analysis reveals that the minimum fuel mass required for stable wall-impinging ignition approximately increases linearly with injection pressure increasing, thus reducing injection pressure and increasing fuel mass help to improve combustion quality and enhance environmental adaptability. Xia [12] et al. conducted experimental analysis on the spray characteristics under different nozzle diameters (100, 300, 350 μm) and injection pressures (60, 100, 140, 180 MPa) within a constant volume bomb to elucidate the effects of key factors such as nozzle diameter, injection pressure, and thermodynamic boundary conditions on fuel spray characteristics and critical characteristics. The 350 μm nozzle, due to its higher injection flow rate, results in a significantly larger spray volume compared to other nozzles, while the spray generated by the 100 μm nozzle is easily affected by the ambient air entrainment movement, thereby enhancing the radial expansion process of the spray. The effect of injection pressure on the liquid-phase fuel length, volume, and spray cone angle is not significant, but it significantly affects the fuel–air mixture process. Even under supercritical conditions, increasing the injection pressure still significantly improves the mixing quality in the downstream region of the spray. In summary, the influence of the injector nozzle diameter on in-cylinder fuel–air mixture and combustion process is not clear, and a universal rule has not yet been summarized. The optimization scheme of injector nozzle diameter needs further improvement. Addressing the above issues, this paper adopts a combined approach of bench experiments and numerical simulation to investigate the mechanism of the injector nozzle diameter on the in-cylinder fuel–air mixture and combustion process, based on high-density and lean mixture characteristic combustion strategy, aiming to provide guidance and suggestions for the selection of injector nozzle diameter in the development of diesel engine combustion systems.

2. Spray Characteristics of High-Efficiency Clean Combustion in Diesel Engines

Traditional diesel engine combustion is a highly complex physicochemical process, where liquid diesel undergoes processes such as droplet formation, collision, breakup, atomization, evaporation diffusion, air entrainment, and mixing after leaving the injector before ignition and combustion can occur. John Dec et al. used the two-dimensional laser Rayleigh scattering (LRS) technique to quantitatively study the concentration fields of gas and liquid phase sprays and the generation of soot in an optical engine, and based on quantitative experimental results, proposed a modern diesel engine combustion process model [13] (Figure 1). After the fuel jet leaves the nozzle, it rapidly atomizes as the spray progresses forward, and high-temperature ambient gas is entrained into the spray,

causing the temperature rise and phase change in the liquid-phase fuel, leading to chemical reactions. A high equivalence ratio premixed flame (Φ~4, T = 825 K) appears at the head of the spray, generating heat to heat up the fuel–air mixture to about 1600 K, contributing to approximately 10–15% of the total heat release. In the mid–late stage of spray development, a high-temperature diffusion flame envelope of 2700 K appears around the entire fuel jet, and combustion products rich in fuel from the spray interior such as CO, UHC, PM are continuously transported to this envelope, where they undergo diffusion combustion (including the generation of CO_2 and H_2O, NOx generation, and oxidation of soot). It can be seen that traditional diesel engine combustion is a predictable combustion, closely related to fuel injection, which is easier to control and more suitable for high-load conditions. However, the inherent nature of heterogeneous combustion inevitably results in NOx and soot emissions. Under the flame lift height downstream, the diesel spray forms a premixed reaction zone with an equivalence ratio close to four, and the premixed combustion products will become the "fuel" for the downstream diffusion combustion process of the spray, including the precursor of soot generation. In other words, the distribution characteristics of equivalence ratio inside the spray at the moment of ignition will affect the total amount of harmful emissions such as soot and the heat release rate of the diffusion combustion process.

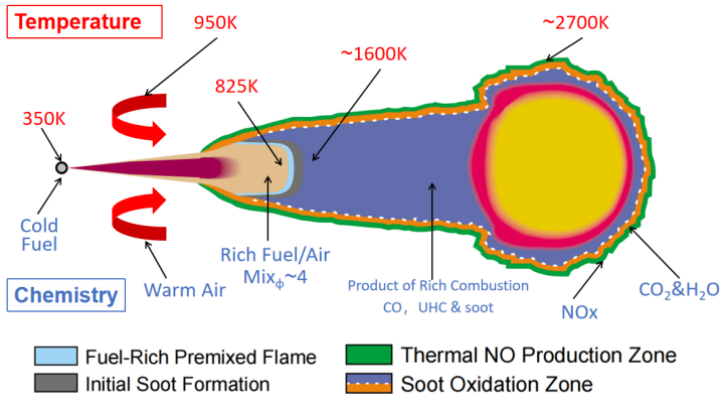

Figure 1. The combustion and emission generation model of traditional diesel engine.

Pickett and Siebers from Sandia National Laboratories in the United States first proposed the concept of leaner lifted flame combustion (LLFC) [14]. By enhancing the air entrainment process within the flame lift height, the equivalence ratio of the mixture in the premixed reaction zone is kept below or equal to 2 (Figure 2), achieving a completely smokeless and relatively low-temperature combustion strategy. The key to achieving the LLFC strategy is to increase the flame lift height and strengthen the spray air entrainment capability. Pickett et al. [14,15] conducted experimental studies in optical constant volume chambers and found that diesel LLFC combustion could be achieved when the ambient temperature and pressure were below specific values. Additionally, reducing the injector nozzle diameter or using oxygen-containing fuels can broaden the operating range of LLFC, as shown in Figure 3. Polonowski et al. [16] found that achieving a continuous smokeless LLFC mode in actual engines is challenging. It requires injection pressures as high as 240 MPa, moderate exhaust gas recirculation rates, and lower intake air temperatures to achieve completely smokeless LLFC with a two-hole injector equipped diesel engine. For injectors with six or more holes, the secondary entrainment of combustion products and the interactions between sprays, making LLFC combustion unsustainable. It is worth noting that the above experimental results were obtained under moderate-load conditions. Achieving LLFC under high-load conditions requires the use of oxygen-containing fuels [17,18], as shown in Figure 4.

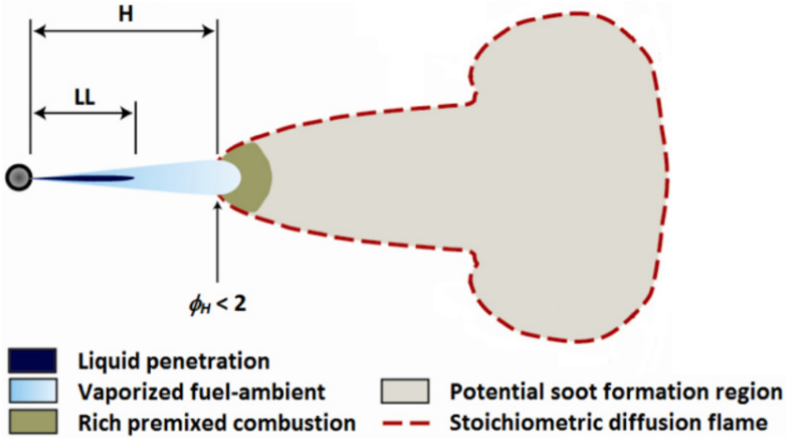

Figure 2. Conceptual model of LLFC combustion strategy.

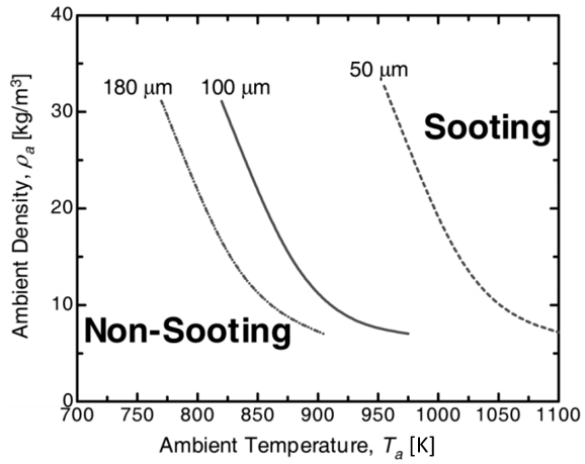

Figure 3. Relationship between soot formation status and injector nozzle diameter in constant volume combustion chamber.

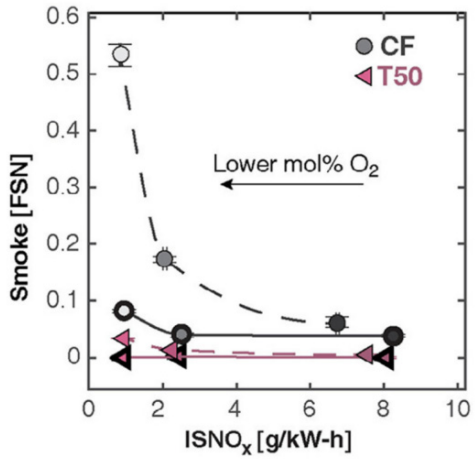

Figure 4. Influence of oxygen-containing fuels on soot and NOx emissions.

In the combustion process of diesel engines, the final amount of soot generated is the result of the combined effects of its formation and oxidation processes. Pursuing combustion processes with zero soot generation is not the only way to address soot emissions. However, in many LLFC test results, excessively low intake air temperatures and oxygen concentrations are used to extend flame lift height, affecting the overall fuel–air mixing process and leading to prolonged combustion duration, sharp increases in HC and CO

emissions levels, and significant reductions in combustion efficiency and engine thermal efficiency. Therefore, simply pursuing combustion modes with flame lift height positions where the mixture equivalence ratio is below two does not meet the requirements of current high-efficiency, clean, low-carbon diesel engines. The inherent uneven mixing of diesel spray leads to a complex distribution of equivalence ratios inside the spray. To determine the relevant reaction pathways, the mixture is divided into different regions based on local fuel–oxygen equivalence ratios: $0 < \Phi < 1$, $1 < \Phi < 2$, and $\Phi > 2$. Different mixtures in different equivalence ratio regions follow specific reaction pathways, as shown in Figure 5. In high-temperature environments above 1400 K, lean mixtures with $0 < \Phi < 1$ directly oxidize to CO_2, releasing a large amount of heat instantly. Rich mixtures with $1 < \Phi < 2$ first generate intermediate product CO, which then reacts with oxygen to form CO_2, with the rate of heat release controlled by the fuel–air mixing rate. Overly rich mixtures with $\Phi > 2$ exceed the equivalence ratio boundary for soot generation. Therefore, lean mixtures with $0 < \Phi < 1$ can complete the combustion heat release process in the shortest time scale, while mixtures with $\Phi > 1$ inevitably undergo the mixing processes, with the mixing time scale far exceeding the chemical reaction time scale, resulting in combustion rates limited by the mixing rate.

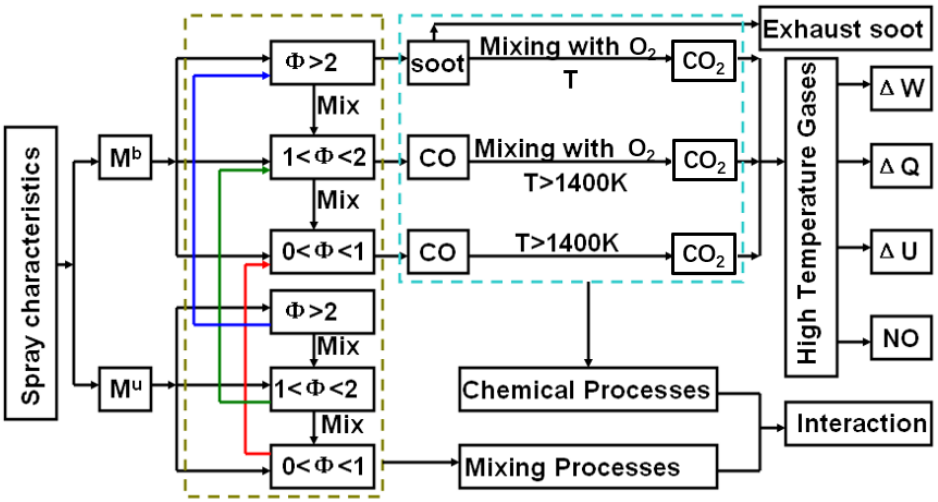

Figure 5. The schematic diagram of spray combustion path of heavy-duty diesel engine.

Diesel spray will form a premixed reaction zone downstream of the flame lift height, where the combustion products in this zone are mainly composed of over-rich mixtures with $\Phi \geq 2$, serving as "fuel" for the downstream diffusion combustion process of the spray. From the analysis of the combustion path, achieving complete combustion of the rich mixture in the premixed reaction zone unavoidably requires a relatively long time scale for the mixing process. It is only through the incomplete combustion product and unburned fuel transport during the fuel–air mixing process that contact with oxygen can achieve complete combustion. At this point, the combustion becomes a mixed-dominated, staged process with a large amount of intermediate product generation. Introducing the Φ–T diagram of CO generation [19] to characterize the combustion efficiency of the diffusion combustion process, it can be seen from Figure 6 that the combustion path curves of diffusion combustion differ significantly at different mixing rates. The smaller the mixing time, that is, the faster the mixing rate, and the further the combustion path is from the CO generation area, indicating that more fuel develops along the lean mixture path throughout the combustion process. At the time scale level that cannot be characterized by the Φ–T diagram, the mixing rate largely affects the duration of diffusion combustion, thereby influencing combustion phase and piston work capacity.

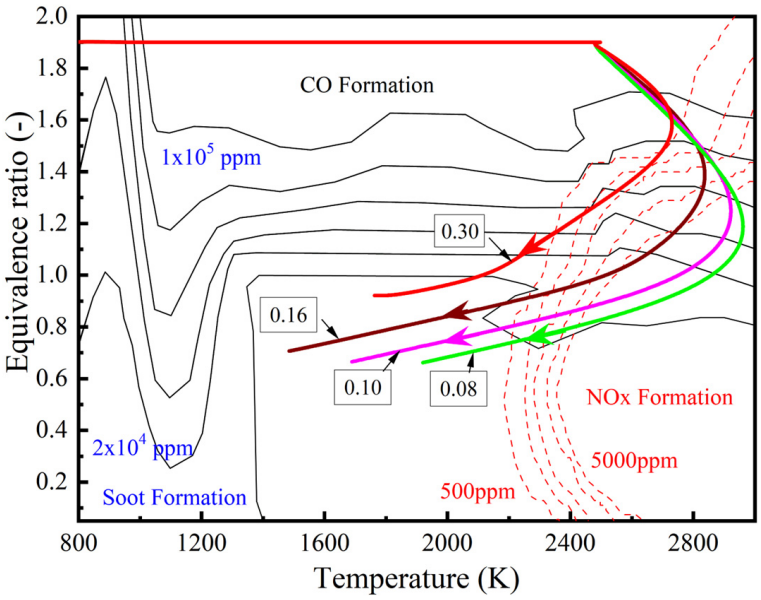

Figure 6. Influence of different mixing rates on the diesel diffusion combustion process.

In summary, the proportion of lean mixtures with $0 < \Phi < 1$ is the most important spray characteristic affecting the overall diesel combustion process. Increasing the proportion of lean mixtures with $0 < \Phi < 1$ inside the spray can enhance the heat release during the premixed combustion stage, and on the other hand, significantly reduce the dependence of the diffusion combustion stage on the mixing rate, making the overall heat release process more concentrated. Ultra-high proportions of lean mixtures are an ideal spray characteristic for efficient and clean combustion. Therefore, increasing the proportion of lean mixtures throughout the ignition timing and the entire spray development process is the key to achieving high-efficiency clean diesel combustion.

3. Test Platform and 3-D Simulation Model

3.1. Single-Cylinder Engine Test Platform

In this study, experiments were conducted on a single-cylinder engine test platform. The original engine parameters are listed in Table 1, and the schematic diagram of a single-cylinder engine test platform is shown in Figure 7. During the experiment, the first cylinder of the original engine was used as the test cylinder. The intake system of the test cylinder used external pressurization combined with intake heating and an independent exhaust gas recirculation system, allowing flexible control of intake pressure, temperature, and EGR rate. In this study, three different injector nozzle diameters were used, with nozzle diameters of 0.169/0.203/0.218 mm. Table 2 shows the parameter settings for the experimental conditions. Table 3 provides specific information on the measurement instruments and their error rates. Single-cylinder exhaust components were detected using a Horiba 7100 exhaust gas analyzer made in Japan, and soot emissions were measured with an AVL 415 smoke meter made in Austria. Cylinder pressure signals were collected using a 6125C cylinder pressure sensor and 5165A charge amplifier by the Kistler company made in Switzerland. The uncertainty of the single-cylinder engine test platform was calculated as follows: Total uncertainty = Square root of {(uncertainty of soot)^2 + (uncertainty of load)^2 + (uncertainty of speed)^2 + (uncertainty of temperature)^2 + (uncertainty of air flow)^2 + (uncertainty of diesel measurement)^2 + (uncertainty of pressure acquisition)^2 + (uncertainty of angle encoder)^2}, and after calculation, the total uncertainty was confirmed to be 1.47%. In addition, cylinder pressure data were measured every 0.5 crank angle degree and the average was taken from 100 consecutive engine cycles. The gaseous emissions and the particulate mass emission were continuously measured for 5 min and the average results

were calculated. The steady-state tests were repeated twice to ensure that the results were repeatable, within the experimental uncertainties of the measurements.

Table 1. Main technical parameters of heavy-duty diesel engine.

Parameter	Value
Cylinder Diameter/mm	116
Stroke/mm	150
Displacement/L	9.5
Compression Ratio	18.5
Intake Swirl Ratio	1.1
Combustion Chamber Shape	Stepped-lip type
Intake Mode	Turbocharged and Intercooled
Rated Power (kW)	294 (at 1900 r/min)
Maximum Torque (N·m)	1800 (1000–1400 r/min)
Maximum Cylinder Pressure (MPa)	24

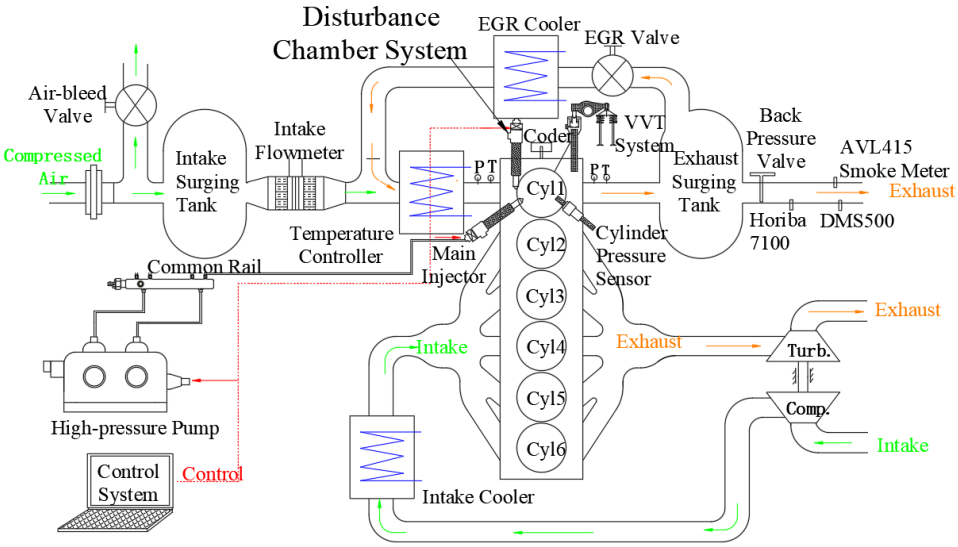

Figure 7. Schematic diagram of single-cylinder engine test platform.

Table 2. Experimental operating conditions parameter.

Parameter	Value	Note
Speed	1200 r/min	Constant
Total Cycle Fuel Mass	180 mg	90% load, constant
Common Rail Pressure	180 MPa	Constant
Fuel Injection Timing	−2~8 deg. ATDC	Variable
Nozzle Diameter	0.169 mm; 0.203 mm; 0.218 mm	Variable
Intake Valve Closing Timing	−100 deg. ATDC (Using RIVCT structure, original engine −150 deg. ATDC)	Constant
Intake Pressure	2.7~4.15 bar	Variable
Intake Temperature	330 ± 3 K	Constant

Table 3. Measuring instruments and error rates.

	Instruments Type	Error
Cylinder pressure sensor	KISTLER 6125C 0–30 MPa	±0.01%F·S
Charge amplifier	5165A	±0.05%F·S
Emission collection equipment	Horiba 7100	±0.1%F·S
Smoke detector	AVL 415	±0.05%F·S
Temperature sensor	PT100 0–700 K	±0.1%F·S
Pressure sensor	0–1 MPa	±0.25%F·S

3.2. Injector Hydraulic System Simulation Model

To simplify the simulation model of the injector hydraulic system, the following basic assumptions are proposed [20]: (1) the rail pressure remains uniformly constant during the injection process; (2) the fuel temperature remains constant during the injection process; (3) the viscosity, density, and elastic modulus of the fuel are considered constant; (4) elastic deformation of the components in the system is not considered; (5) leakage caused by machining issues in flat and conical seals and its effect on chamber pressures are not considered. The following equations form the mathematical model describing the dynamic process of the hydraulic system [21]:

(1) The internal pipes of the injector are treated as concentrated volumes, and fuel flow follows the law of mass conservation

$$Q_{gi} = Q_{go} + \frac{V_g}{E} * \frac{dp_g}{dt}, \tag{1}$$

where Q_{gi} is the flow into the pipe, Q_{go} is the flow out of the pipe, V_g is the pipe volume, E is the elastic modulus of the fuel, p_g is the fuel pressure inside the pipe, and t is time.

(2) The influence of the shape of the control chamber and pressure-bearing groove on the operation of the injector can be neglected, and the volume is the main influencing factor. It can be expressed as a volume chamber model, and fuel flow follows the law of mass conservation

$$\sum Q_i = \frac{V_i}{E} * \frac{dp_i}{dt} + \frac{dV_i}{dt}, \tag{2}$$

where Q_i is the change in flow rate in the i volume chamber, V_i is the volume of the i volume chamber, p_i is the pressure inside the i volume chamber, and t is time.

(3) Treating the control rod and needle valve as a whole, according to Newton's second law, the motion equation of the needle valve is

$$m\frac{^2x}{t} = F_C + F_y + F_z - F_k - k(xo + x), \tag{3}$$

where x is the lift of the needle valve, m is the total mass of the control rod and needle valve, F_c is the force of the fuel on the needle valve at the pressure-bearing groove, F_y is the force of the fuel on the needle valve at the pressure chamber, F_z is the supporting force at the needle valve seat, F_k is the force of the control chamber on the control rod, k is the stiffness of the needle valve spring, and x_0 is the preload of the needle valve spring.

Based on the above mathematical model, a simulation model of the injector hydraulic system is built in the AMESim 2020 simulation platform, as shown in Figure 8. To verify the accuracy of the simulation model, the actual fuel injection rate is measured using the EFS high-pressure common rail test bench. The test was carried out under the conditions of 180 MPa common rail pressure and 1.5 ms pulse width. After filtering and shaping, the measured fuel injection rate matches well with the simulated fuel injection rate under the same conditions, as shown in Figure 9. This indicates that the simulation results can reflect the actual fuel injection pattern, and the simulation model of the high-pressure common rail injector hydraulic system is reliable.

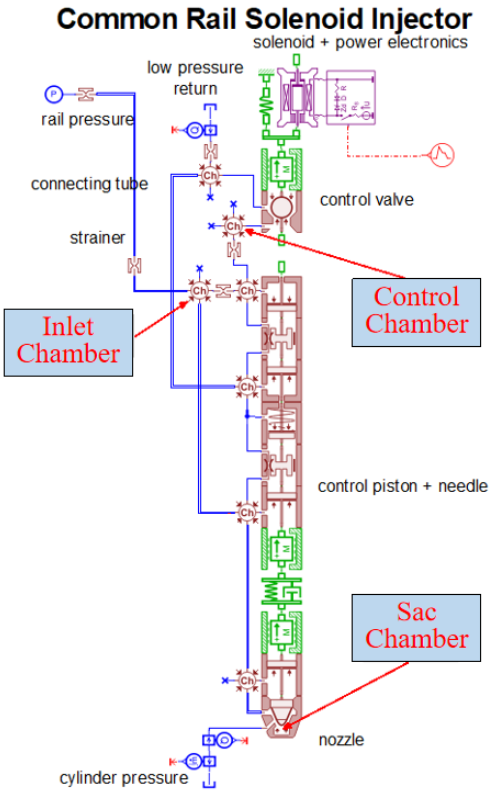

Figure 8. Simulation model of high-pressure common rail injector hydraulic system.

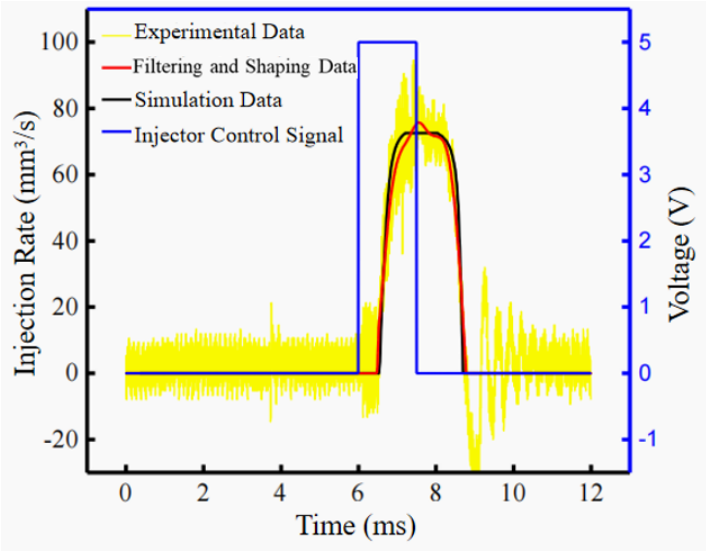

Figure 9. Comparison of fuel injection rate experimental results and simulation results.

3.3. 3-D Combustion Simulation Model

Based on the geometric parameters of the combustion chamber, modeling will be carried out using Solidworks 2023. Since the original engine combustion chamber is a rotationally symmetric regular revolving body, and the eight injector nozzles are evenly distributed circumferentially, a one-eighth combustion chamber will be used for simulation to improve computational speed. Three-dimensional simulation models were established based on the computational fluid dynamics software CONVERGE 2.3 (Figure 10), with a base grid size of 4.0 mm. The important mathematical models used in the simulation calculations are shown in Table 4.

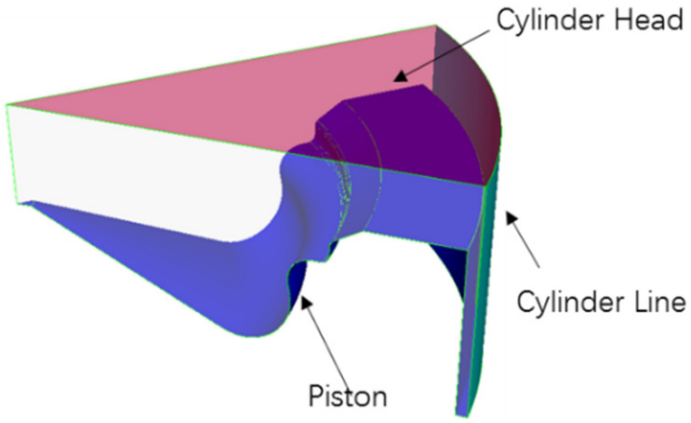

Figure 10. Geometric model of the combustion chamber.

Table 4. Models used in simulation calculations.

Parameter	Value
Turbulence Model	RNG k-ε
Combustion Model	SAGE Chemical Reaction Solver + Simplified Chemical Reaction Kinetics Mechanism
Heat Transfer Model	Han and Reitz
Spray Breakup Model	KH-RT
Spray Wall Impact Model	O'Rourke and Amsden
Droplet Collision Model	NTC collision
Spray Evaporation Model	Frossling
Base Grid Size/mm	4

Based on the obtained experimental data, the simulation model was calibrated and validated. The calibration condition had an intake pressure of 4.15 bar and an injection timing of −2 deg. ATDC, with other test conditions referenced from Table 2. The simulation results for injectors with different nozzle diameters were compared with actual experimental results, as shown in Figure 11. Comparing the simulation results with the experimental results, the peak cylinder pressure error was less than 0.1%, the crank angle error corresponding to the peak cylinder pressure was less than 0.5 deg, and the peak heat release rate error was less than 2%. It can be considered that the simulated data closely matches the experimental data, and the established simulation model can be used to accurately describe the combustion process of the diesel engine.

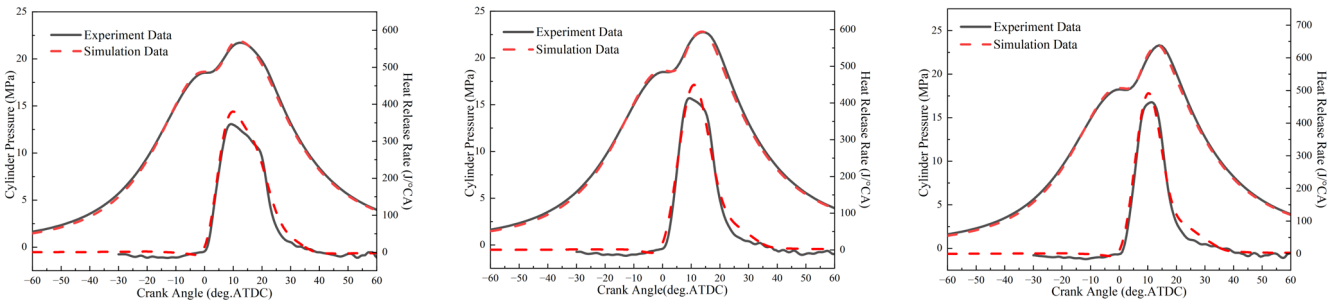

(**a**) (**b**) (**c**)

Figure 11. Comparison of cylinder pressure and heat release rate between simulation and experiment: (**a**) 0.169 mm; (**b**) 0.203 mm; (**c**) 0.218 mm.

4. Results and Discussion

4.1. Experimental Study on the Influence of Injector Nozzle Diameter on Combustion Process

Experimental research on the influence of the injector nozzle diameter on combustion and emissions was conducted based on the aforementioned test platform. Figure 12 presents experimental data including cylinder pressure, instantaneous heat release rate, and average in-cylinder temperature for three injector nozzle diameters at an intake pressure of 4.15 bar and a rail pressure of 180 MPa. The injection strategy was single injection, and the injection start time was −2 deg. ATDC. As the injector nozzle diameter increases from 0.169 mm to 0.218 mm, the maximum cylinder pressure increases, and the combustion heat release process becomes more intense and concentrated. The peak heat release rate increases by 33.9%, and the combustion duration shortens from 26.3 deg to 20.8 deg. Additionally, both the combustion center CA50 and the combustion end CA90 move closer to the top dead center. Furthermore, observation of the average in-cylinder temperature reveals that increasing the injector nozzle diameter leads to a greater temperature rise during the combustion process, with the timing of the temperature peak significantly advancing.

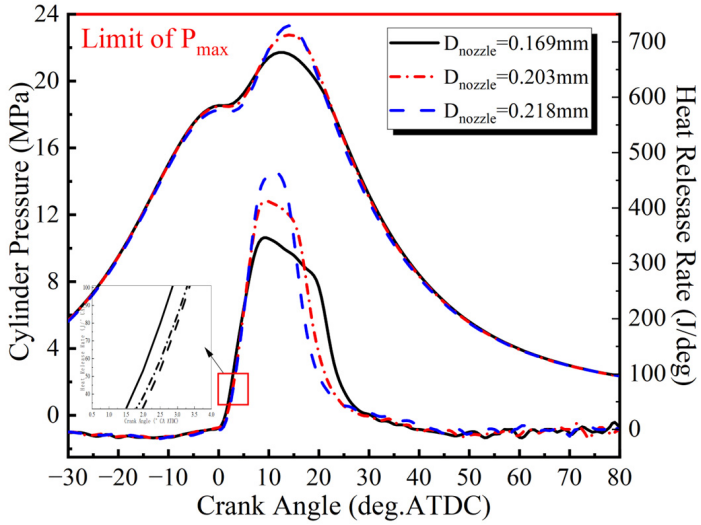

(**a**)

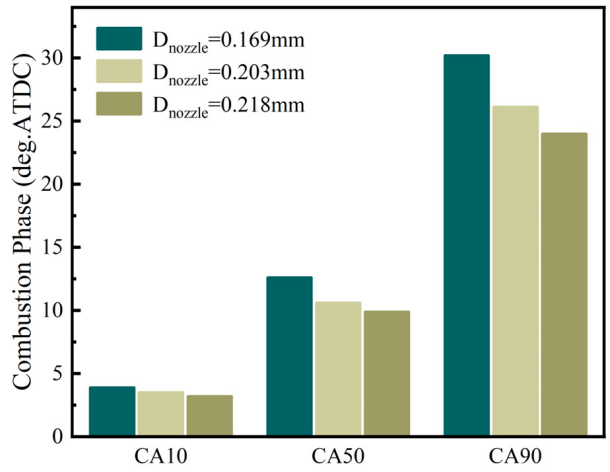

(**b**)

Figure 12. *Cont.*

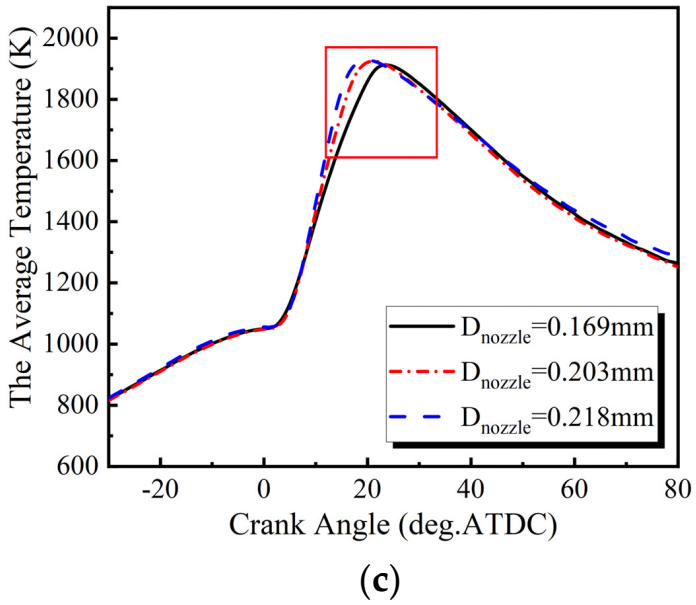

Figure 12. Combustion characteristic parameters corresponding to three injector nozzle diameters: (**a**) cylinder pressure and heat release rate; (**b**) combustion phase; and (**c**) average temperature.

Figure 13 illustrates the impact of injector nozzle diameter on major harmful emissions. Experimental results indicate that there is little difference in the emissions of CO, soot, and UHC for different nozzle diameters. The original emissions of CO and soot from the engine are much lower than the emission limits corresponding to the WHSC test cycle in the Euro VI emission standard. The original emission of UHC is close to the aforementioned emission limit. When the nozzle diameter increases from 0.169 mm to 0.218 mm, the NOx emissions exhibit a trend of first increasing and then decreasing. This is because increasing the nozzle diameter leads to a greater temperature rise in the cylinder during diesel combustion, resulting in an increase in NOx production. However, when the nozzle diameter increases to 0.218 mm, the overall combustion duration shortens by 20%, and the duration of high-temperature NOx generation elements also decreases accordingly, leading to a reduction in NOx emissions.

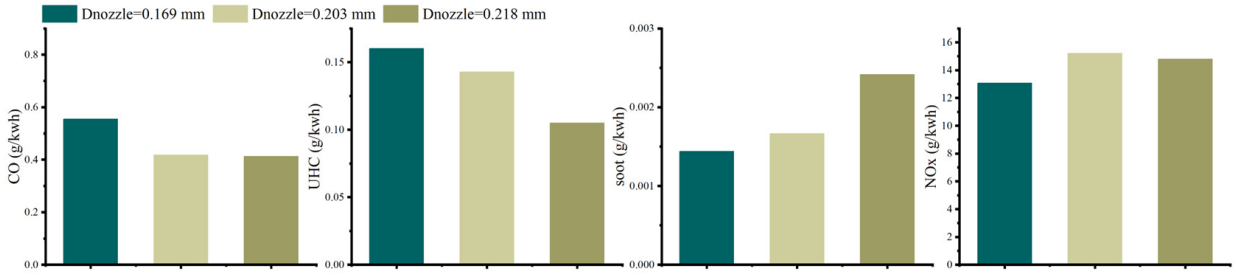

Figure 13. Influence of injector nozzle diameter on major harmful emissions.

Figure 14 shows the influence of the injector nozzle diameter on energy loss distribution. As the nozzle diameter increases, the heat transfer loss initially increases and then decreases. This is mainly due to the increase in the nozzle diameter, which significantly increases the cylinder temperature and average pressure during diesel combustion, affecting the temperature difference and heat transfer coefficient in the wall heat transfer process, resulting in an increase in wall heat transfer rate. However, on the other hand, the 20% reduction in combustion duration reduces the duration of high-temperature in-cylinder, so under the interplay of these two factors, heat transfer loss exhibits a trend of initially increasing and then decreasing with the increase in nozzle diameter. The increase in nozzle diameter increases the proportion of constant volume combustion, allowing for a more

thorough expansion of the working fluid and reducing exhaust temperature. Consequently, exhaust loss decreases monotonically with the increase in nozzle diameter. Benefiting from the simultaneous reduction in heat transfer loss and exhaust loss, indicated thermal efficiency increases with the increase in nozzle diameter. Under the condition of 1200 rpm and IMEPg of 2.3 MPa, using a nozzle diameter of 0.218 mm, the indicated thermal efficiency reaches as high as 51.5%.

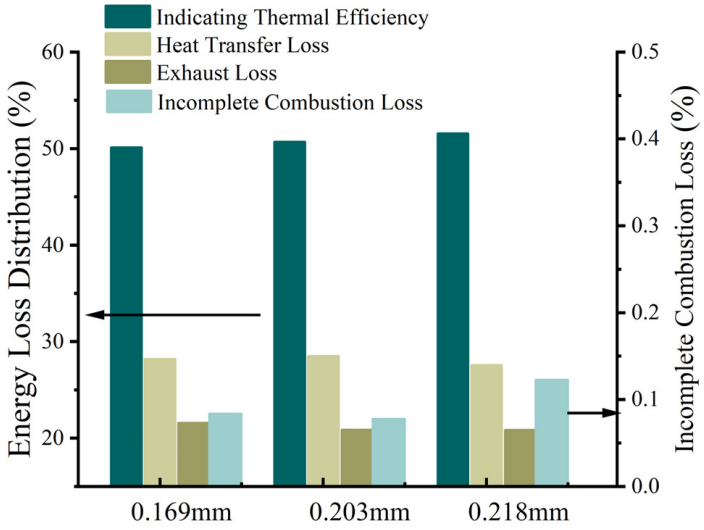

Figure 14. Influence of injector nozzle diameter on energy loss distribution.

Based on the comprehensive analysis of the test results, under the thermodynamic boundary conditions in this study, as the nozzle diameter increases from 0.169 mm to 0.218 mm, the combustion process of diesel becomes more rapid, with a 20% reduction in the duration of combustion. Furthermore, the combustion is sustained for a shorter period, and the proportion of constant volume combustion increases. Indicated thermal efficiency at high-load conditions also rises from 49.8% to 51.5%. While the experimental results provide insights at a macroscopic level into the impact of nozzle diameter on heat release rate, thermal efficiency, and emissions, a microscopic understanding of the variation in nozzle diameter on in-cylinder fuel–air mixture and combustion processes is lacking. The following sections will utilize numerical simulation methods to analyze in-cylinder spray air entrainment motion and the distribution of mixed gas within the spray, aiming to elucidate the influence mechanism of nozzle diameter on the combustion process from the perspective of fuel–air mixture.

4.2. Influence of Nozzle Diameter on Spray Internal Mixing Quality

Changes in nozzle diameter affect the pressure fluctuation characteristics inside the injector, but the range of pressure fluctuation is mainly influenced by the effective injection pressure. Therefore, it is necessary to focus on the impact of nozzle diameter on the pressure loss characteristics inside the injector. Three injectors used in the experiments were simulated in the AMESim model to analyze the effects of nozzle diameter on effective injection pressure and actual fuel injection rate. It should be noted that the three injectors used in this study are all conical hole nozzles, with a nozzle coefficient K of 0.5. The coefficient K is defined as $(D_{inlet} - D_{outlet})/10$. Previous studies [22] have shown that when $K > 0$, it indicates that the nozzle along the flow direction is contracting, which will significantly inhibit the geometrically induced cavitation process inside the nozzle. Therefore, this study does not consider the influence of cavitation process inside the nozzle.

Friction in the internal pipeline, pipeline diameter switching, connection points, and the opening position of the needle valve of the fuel injection system all contribute to fuel pressure loss, ultimately leading to an actual fuel injection pressure much lower than the pressure inside the common rail. Figure 15a shows the pressure distribution and the form

of pressure loss at various positions inside the injector when the needle valve is fully open. Along-the-way loss refers to the energy loss caused by fuel flow friction with the pipe wall in a straight pipe, mainly occurring in the external high-pressure fuel pipe and the internal high-pressure fuel passage. There are also local pressure losses inside the injector, including sudden expansion and sudden contraction of the pipeline, especially at the needle valve. Changes in the nozzle diameter affect the local resistance coefficient between the sac chamber and the nozzle, but the greater influence on effective injection pressure is its effect on the flow rate of the entire high-pressure fuel passage. The flow velocity of fuel in the entire fuel injection system increases, and both the along-the-way loss and local loss in the internal fuel injection system significantly increase, leading to a significant decrease in effective injection pressure, as shown in Figure 15. For the three nozzle diameter injectors, under the common rail pressure of 180 MPa and the cycle fuel mass quantity of 180 mg, the average injection pressure within a single injection cycle is 131, 105, and 94 MPa (0.169 mm/0.203 mm/0.218 mm), respectively.

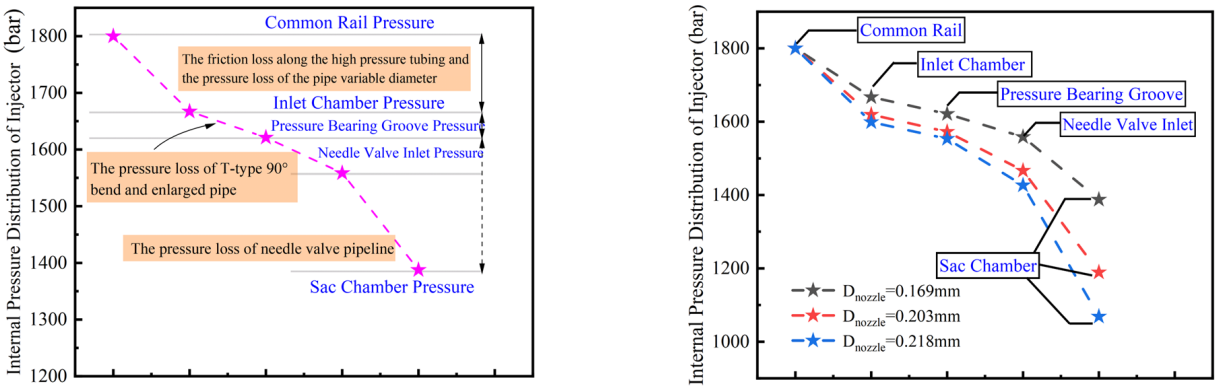

Figure 15. Pressure loss characteristics inside the injector: (**a**) pressure loss forms at various positions inside the injector; (**b**) pressure distribution at various positions inside different diameter injectors.

The change in the nozzle diameter from 0.169 mm to 0.218 mm will result in alterations in both the internal pressure loss of the injector and the cross-sectional area at the nozzle outlet, inevitably affecting the actual fuel injection rate. According to the Bernoulli equation, the fuel flow rate through the nozzle can be expressed as follows:

$$\dot{m}_f = \int Au \cdot \rho dA = A\sqrt{2\Delta p(t)\rho} = \frac{\pi}{4} d^2 \sqrt{2\Delta p(t)\rho}, \quad (4)$$

where $\Delta p(t)$ is the pressure difference between the inlet and outlet of the nozzle; A is the cross-sectional area at the nozzle outlet; ρ is for the density of the diesel used in the experiment; and $\dot{m}_f$ is the mass flow rate at the nozzle outlet. Figure 16 illustrates the fuel injection rate corresponding to different nozzle diameters under a fixed injection pulse width. The fuel injection rate curves exhibit a trapezoidal pattern, which is quite similar to the lift curve of the needle valve. This resemblance is primarily due to the influence of the constrained area formed between the needle valve and its seat on the fuel injection rate. When the needle valve reaches its maximum lift, the fuel injection rate peaks. After 0.003 s from the start of injection, the fuel injection rate stabilizes relatively. At this point, the fuel injection rates corresponding to the three nozzle diameters, from smallest to largest, are 5.28 L/min, 6.70 L/min, and 7.23 L/min, respectively. Under the condition of 180 MPa common rail pressure and a cycle fuel mass of 180 mg, the durations of fuel injection for the respective nozzle diameters are 2950 ms, 2370 ms, and 2180 ms.

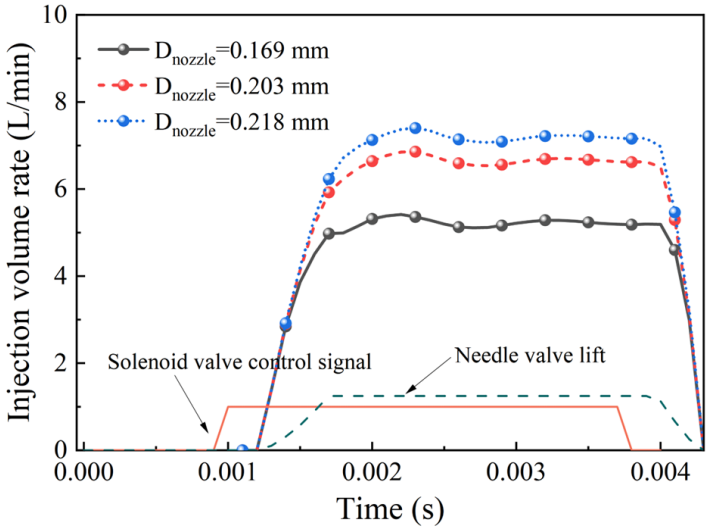

Figure 16. Influence of injector nozzle diameter on actual fuel injection rate.

The momentum of spray ejected will affect the subsequent evaporation and mixing quality of the spray in-cylinder, thereby influencing the final combustion process and emissions. The momentum of the spray at the nozzle outlet can be defined as follows:

$$\dot{M}_f = \int Au^2 \cdot \rho dt = 2A \cdot \int \Delta p(t) dt = \frac{\pi}{2} d^2 \int \Delta p(t) dt, \quad (5)$$

where $\dot{M}_f$ is the momentum of spray at the nozzle outlet within a fixed time step. To calculate the momentum of spray ejection, it is necessary to determine the statistical time step. In this study, a unit time step of 1×10^{-5} s was chosen. Increasing the injector nozzle diameter results in a decrease in actual injection pressure and fuel ejection velocity. However, increasing the injector nozzle diameter significantly improves the fuel injection rate. These two factors combined result in an increase in the average momentum of spray ejection per unit time from 3.25 kg·m/s to 4.21 kg·m/s as nozzle diameter increases when the needle valve is fully open, as shown in Figure 17. However, when cumulative momentum of spray ejection is calculated for a fixed total cycle fuel injection mass, it is found that due to differences in the duration of fuel injection, the cumulative momentum of spray ejection for smaller nozzle diameters actually increases.

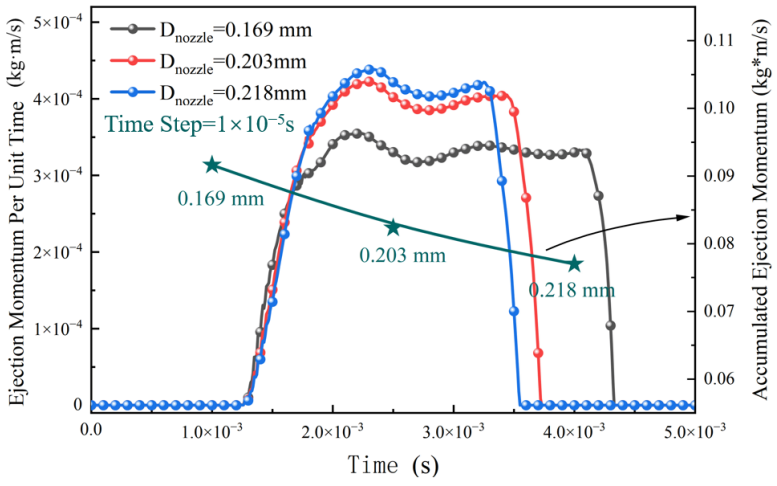

Figure 17. Influence of injector nozzle diameter on fuel ejection momentum.

The phenomenon of air entrainment during the development of fuel spray is a crucial physical process. The high-temperature air entrained into the spray promotes the evapora-

tion of liquid fuel by exchanging energy with the fragmented liquid droplets. Additionally, the motion of air entrainment determines the mixing quality between fuel and fresh air during spray development. Therefore, the quantity and velocity of air entrainment during spray development are important factors affecting the overall combustion performance of diesel engines. The strength of air entrainment during the free development of the spray depends on the rate of momentum exchange between the spray and the ambient gas. Within the range of injector diameters studied, the momentum of spray ejected per unit time increases with the increase in nozzle diameter, and the momentum entering the cylinder space per unit time should also increase synchronously. After high-speed spray enters the cylinder, its momentum density distribution exhibits a spindle-shaped layered structure, with the spray core area near the nozzle outlet having the highest momentum density, as shown in Figure 18. With the increase in nozzle diameter, the axial penetration speed of the spray increases, and the axial range of the high momentum density region expands. While the spray develops axially, the spray edges experience frictional shearing with the air, resulting in intense momentum exchange at the spray edges. To quantify the radial momentum transfer of the spray, the kinetic energy of the core and non-core regions at various axial positions of the spray was statistically analyzed, where the core region is defined as a cylinder with the nozzle axis as the axis and the nozzle diameter as the bottom diameter. As shown in Figure 19, increasing the nozzle diameter significantly increases the total kinetic energy at various axial positions of the spray, enhances the spray penetration rate, intensifies the frictional shearing between the spray and ambient air, improves the momentum exchange capability, and increases the proportion of kinetic energy transferred from the upstream region of the spray to the non-core region from 53% to 59%. As a result, the radial expansion of the spray increases.

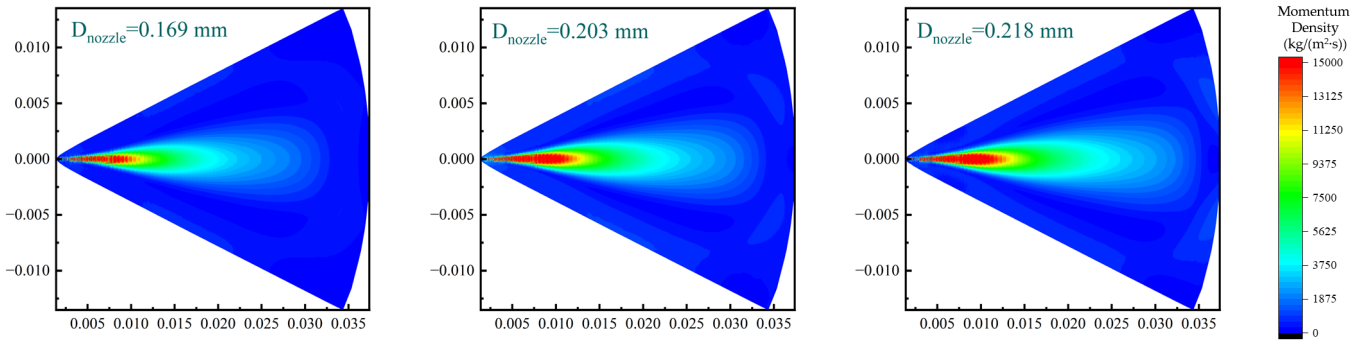

Figure 18. Momentum density distribution contour under three nozzle diameters.

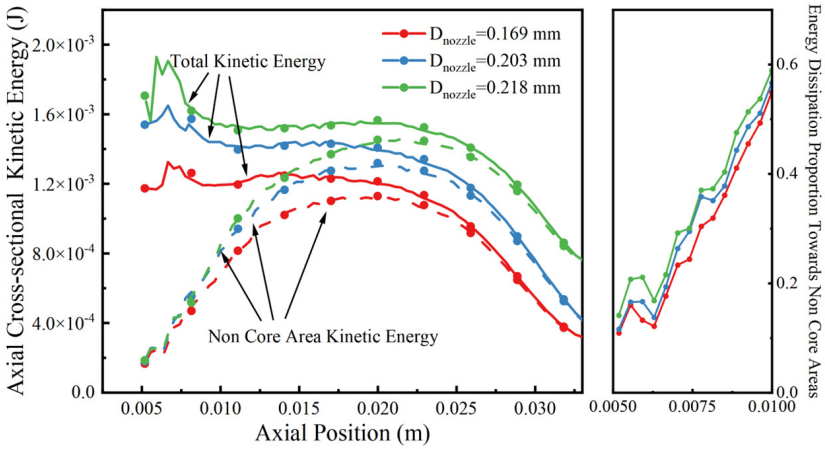

Figure 19. Axial cross-sectional kinetic energy and energy dissipation ratio at various positions under three nozzle diameters.

Figure 20 illustrates the characteristics of flow field distribution in the near and far fields of the spray under different nozzle diameters before spray/wall impingement (5.5 deg. ATDC). From the figure, it can be observed that while diesel spray develops axially, its front end pushes fresh air to both sides of the spray, and under the action of pressure difference, air from the sides enters the interior of the spray. The process of air entrainment by the spray mainly occurs at the middle and upper positions of the spray, and the air entrainment effect at the middle position of the diesel spray is most significant. As the spray develops axially forward, the momentum transferred to the radial air gradually increases, while the corresponding penetrating momentum gradually decreases. Ultimately, under the combined action of upstream spray and ambient gas, the mixture of spray far from the axis stops forward penetration and undergoes lateral movement, and under the action of pressure difference, flows backward upstream, defining this region as the "recirculation zone" where the outflow of fresh charge equals the inflow. Analyzing the velocity field near the edges of the spray under different nozzle diameters, both in the near and far fields, the airflow velocity increases with the increase in nozzle diameter. Statistically, the average air velocities near the spray edges corresponding to nozzle diameters from small to large are 7.67 m/s, 9.69 m/s, and 9.85 m/s in the near field, and 9.75 m/s, 11.71 m/s, and 11.93 m/s in the far field. The airflow velocity of the spray depends on the momentum flux transferred from the spray to the air radially. From the above study, it can be inferred that increasing the injector nozzle diameter increases the momentum ejected per unit time by the spray, increases the total momentum transferred to the surrounding gas, intensifies the mass transfer entrainment process at the spray edge, and increases the lateral airflow velocity near the spray edges.

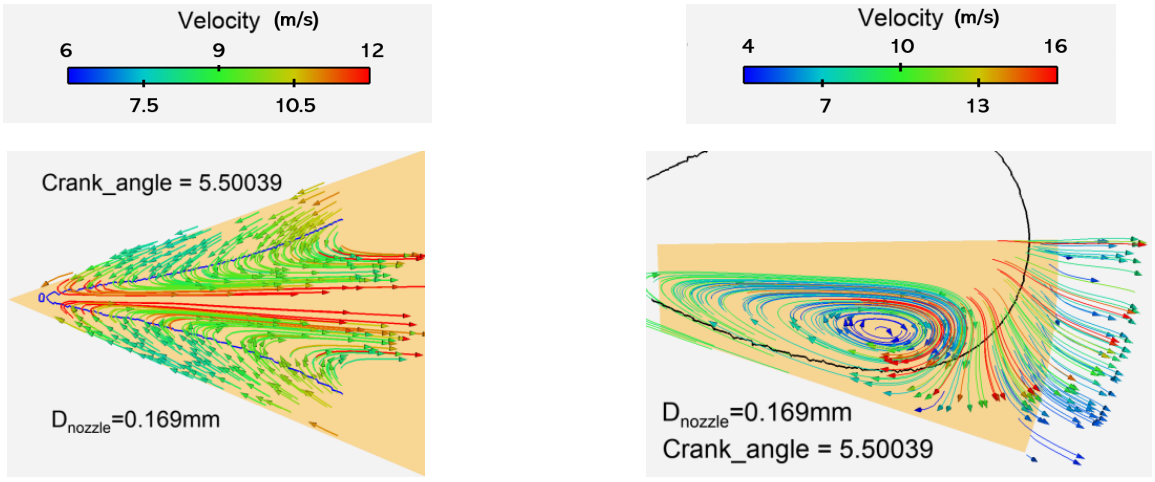

(**a**)

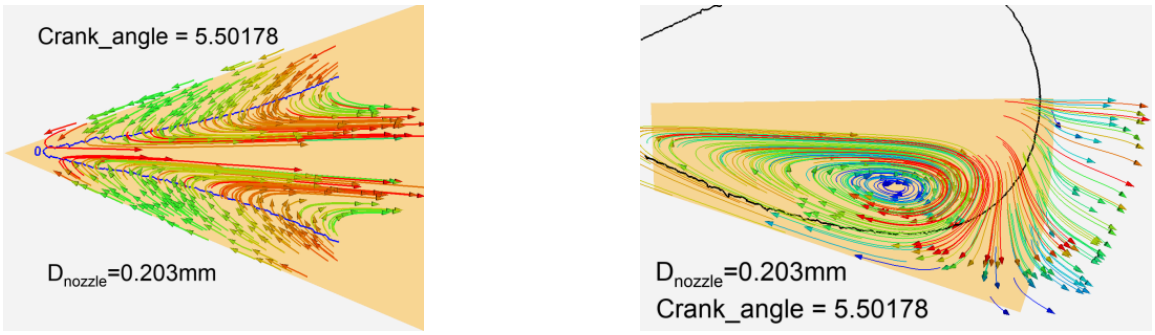

(**b**)

Figure 20. *Cont.*

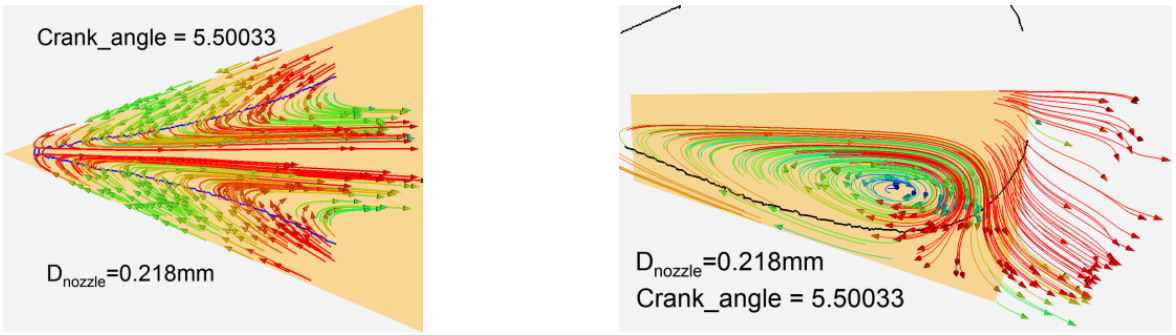

(**c**)

Figure 20. Distribution flow fields in the near and far fields of the sprays under three injector nozzle diameters (5.5 deg. ATDC): (**a**) 0.169 mm; (**b**) 0.203 mm; (**c**) 0.218 mm.

High airflow velocity does not necessarily imply more efficient oxygen transport. It is also necessary to consider the relationship between flow direction and spray, as well as the concentration gradient of input substances. Therefore, Dr. Zhang from Tianjin University proposed the oxygen transport rate α to measure the strength of oxygen transport during the free development process of the spray [23]. This parameter comprehensively considers the direction of airflow and the concentration gradient of input substances. It is defined as follows:

$$\alpha = \vec{V} \cdot \nabla O_2 = \left|\vec{V}\right| |\nabla O_2| cos\theta, \tag{6}$$

That is a detailed explanation of the oxygen transport rate α, defined as the dot product between the flow direction and the gradient of oxygen mass fraction. θ is the angle between the velocity vector and the gradient vector of oxygen mass fraction. When the angle θ is less than 90° (approximately indicating the same direction), $\alpha > 0$; when the angle is greater than 90°, $\alpha < 0$.

Figure 21 presents the distribution of oxygen transport rate in the cylinder under three different nozzle diameters at 5.5 deg. ATDC. It can be observed from the figure that during the free development process of the spray, oxygen is primarily transported along the concentration gradient into the spray, with a large amount of oxygen entering the interior of the spray. The oxygen transport rate is high in the region near the nozzle outlet, and as the spray moves away from the nozzle outlet, the concentration gradient between the spray edge and the surrounding environment as well as within the spray decreases significantly, leading to a decrease in transport rate. Meanwhile, the distribution of high transport rate regions also changes. Unlike the upstream where the entire spray has globally high transport rates, the oxygen transport in the middle region of the spray mainly occurs between the spray edge and the spray core region due to the large oxygen concentration gradient in that area. The spray core region closer to the axis does not have effective oxygen transport due to low oxygen concentration gradients and high axial penetration speeds. Figure 22 shows the distribution of transport rates at various positions on two radial sections, X = 0.1 m and X = 0.2 m, representing the upstream and midstream of the spray, respectively. The oxygen transport in the upstream of the spray is undergoing intense motion with a bimodal distribution, while the oxygen transport distribution in the midstream differs significantly from the upstream. Although it also shows a bimodal distribution, there is no effective oxygen transport near the nozzle axis. With increasing nozzle diameter, the oxygen transport rate in the upstream and midstream of the spray significantly increases, intensifying the entrainment motion of ambient air into the spray and promoting the mixing and combustion processes.

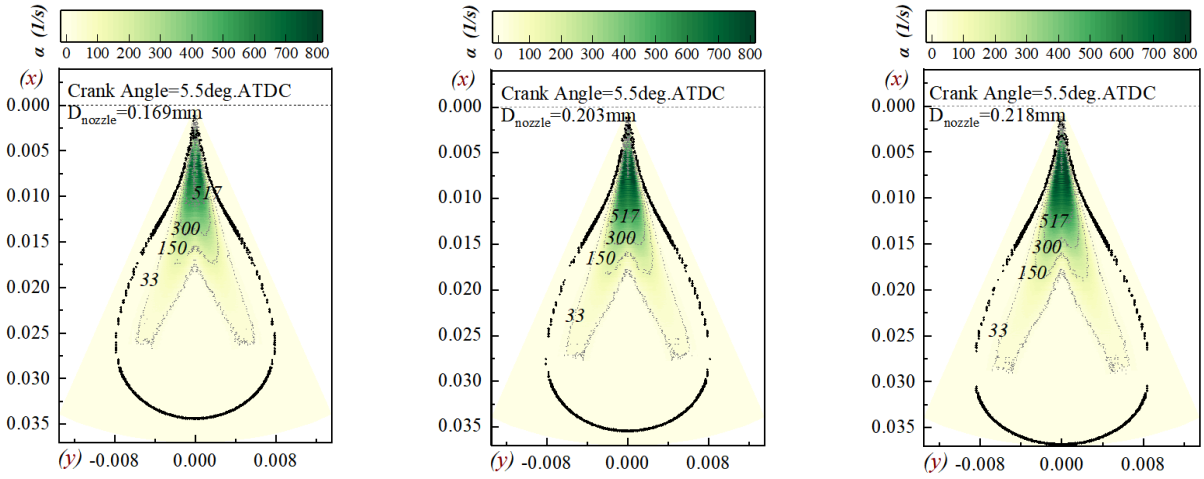

Figure 21. Distribution of oxygen transport rate under three injector nozzle diameters (5.5 deg. ATDC).

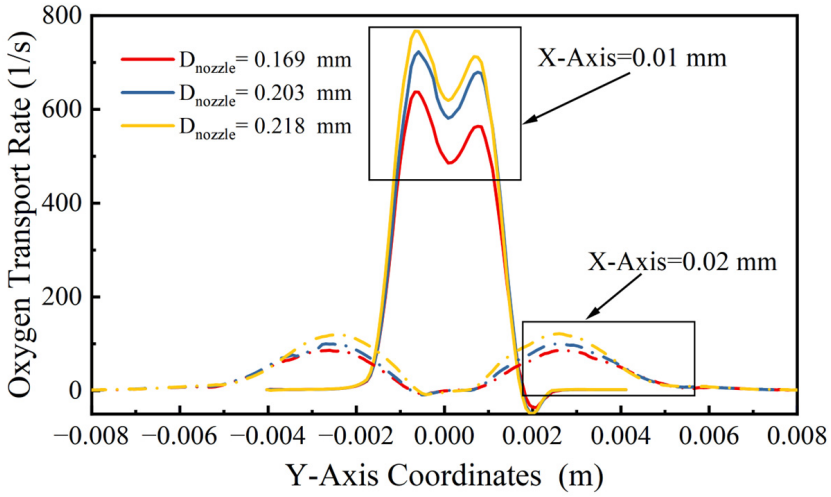

Figure 22. Distribution of oxygen transport rates at various positions on two radial sections of spray under three injector nozzle diameters (5.5 deg. ATDC), X = 0.1 m and X = 0.2 m.

Coupled time series statistically analyzed the cumulative air entrainment mass by the spray at different times, as shown in Figure 23. The air entrainment mass by the spray monotonically increases with the injection time, and the rate of increase continues to rise until the spray/wall impingement. When the spray develops to the piston wall, the effective entrainment area of the spray during the free development stage will no longer increase. Additionally, the fuel impinging on the wall will be guided by the wall to move in the opposite direction from both sides of the spray, which will have a negative effect on the air entrainment during the free development stage. Therefore, the impingement of the spray on the wall is the turning point of the rate of change of air entrainment mass, and its peak appears near the moment of spray/wall impingement. As the nozzle diameter increases from 0.169 mm to 0.218 mm, the air entrainment mass by the spray significantly increases in the same spray development time. Although increasing the nozzle diameter may lead to an earlier spray/wall impingement time, from the perspective of air entrainment mass at the impingement time, the larger nozzle diameter still has advantages. The air entrainment mass at the impingement time corresponding to a nozzle diameter of 0.218 mm is 1.42 times that of 0.169 mm.

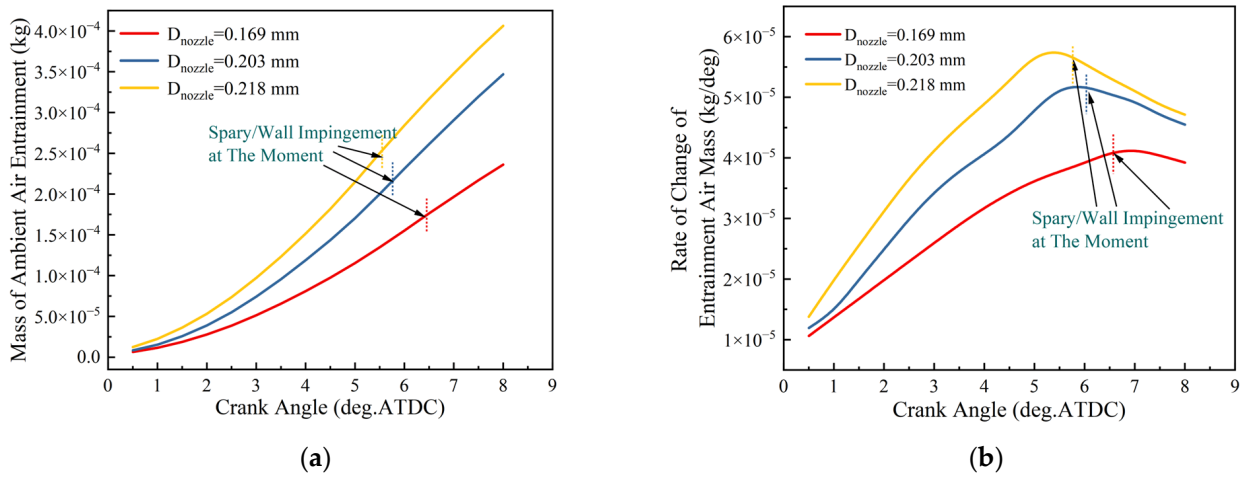

(**a**) (**b**)

Figure 23. The variation of entrained air mass and its rate of change with injection time under different nozzle diameters: (**a**) air entrainment mass; (**b**) rate of change of air entrainment mass.

Earlier analysis of the combustion path of diesel engines revealed that the proportion of lean mixtures ($0 < \Phi < 1$) plays a crucial role in the overall diesel combustion process, with an ultra-high lean mixture ratio being ideal for efficient and clean combustion. However, the concentration field distribution inside the spray is non-uniform, and different regions within the spray exhibit different mixing characteristics. Taking a nozzle diameter of 0.169 mm as an example (Figure 24), in the region from the nozzle outlet to the ignition boundary (0–0.005 m), the high-temperature air entrained into the spray exchanges energy with the fragmented liquid droplets, thereby promoting droplet evaporation. In this region, the evaporation rate of liquid-phase fuel is significantly higher than the air entrainment rate. Consequently, the phenomenon of $\Phi > 1$ mixtures reaching peak values in ascending order of equivalence ratio intervals is observed. Wherein, the mass fraction of mixtures with $\Phi > 4$ continuously increases and eventually reaches 50%. In the region from the ignition boundary to the maximum liquid length (0.005–0.015 m), air entrainment gradually reaches a balance with fuel evaporation and even dominates. The mass fraction of mixtures with $\Phi > 4$ first stabilizes and then rapidly decreases. Notably, the decrease in mixtures with $\Phi > 4$ does not lead to a significant increase in mixtures with $1 < \Phi < 3$; instead, there is a substantial increase in the proportion of lean mixtures with $\Phi < 1$. In the region from the maximum liquid length to the spray head (>0.015 mm), the liquid-phase fuel has completely evaporated, while air entrainment continues. The equivalence ratio in the core region of the spray gradually decreases. Coupled time series comparison of the mass fractions of lean mixtures with $\Phi < 1$ and rich mixtures with $\Phi > 1$ under different injector nozzle diameters (Figure 25) reveals that in the early stage of injection, the mass fraction of rich mixtures corresponding to larger nozzle diameters is higher, indicating more liquid-phase fuel has evaporated, which is beneficial for subsequent fuel–air mixing. As the injection progresses, the proportion of liquid fuel that has evaporated inside the spray continuously increases, leading to an increase in the mass fraction of lean mixtures. At the moment of ignition, the mass fractions of lean mixtures corresponding to the three nozzle diameters are comparable, with approximately 52%. Larger nozzle diameters change the fuel injection rate, leading to an increase in the total amount of fuel entering the cylinder at the moment of ignition, thereby synchronously increasing the mass fraction of lean mixtures with $\Phi < 1$. The mass fraction of lean mixtures inside the spray reaches its peak value at the moment of impingement. The mass fractions of lean mixtures corresponding to the three nozzle diameters, from smallest to largest, are 60.2%, 62.7%, and 64.0%, respectively. Hence, increasing the nozzle diameter can increase the proportion of lean mixtures inside the spray during the free development stage, thereby enhancing the rate of heat release during the free development stage.

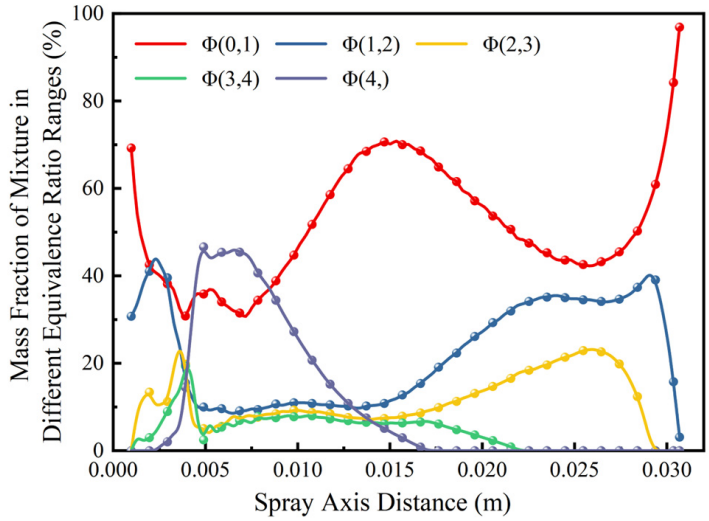

Figure 24. Mass fraction of mixture in different equivalence ratio range (0.169 mm 5.5 deg. ATDC).

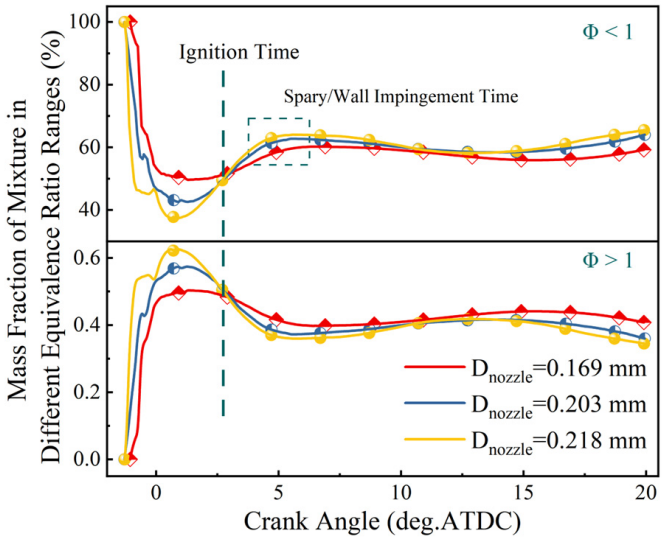

Figure 25. Mass fraction of mixture in different equivalence ratio ranges under three injector nozzle diameters.

Owing to the increase in spray momentum at the nozzle outlet, the friction and shear effects between the spray and fresh air become more pronounced during the axial penetration development process. As the injector nozzle diameter increases, the proportion of momentum transferred radially in the core region of the spray upstream becomes higher. The increase in the total momentum coupled with the increase in the dissipation ratio, results in an increase in the momentum transferred to the fresh air by the spray radially. Consequently, the overall oxygen transport process within the spray becomes more intense, the air entrainment rate significantly increases, and the accumulated air entrainment mass during the free development stage increases. This leads to an improvement in the mixture quality inside the spray, an increase in the proportion of lean mixtures, and an acceleration of the heat release during the free development stage of the spray combustion. However, it is noteworthy that, under the operating conditions considered in this study, over 70% of the combustion process is accompanied by spray/wall impingement. After spray/wall impingement, the mixing rate between the spray and air is significantly reduced due to momentum loss, and the limited fuel–air contact area slows down the fuel heat release rate, affecting the overall combustion quality. Therefore, it is necessary to discuss the influence of the wall-attached fuel mixing rate. In this study, a stepped-lip combustion chamber was used, which replaces the protruding lip of the traditional reentrant ω-shaped combustion

chamber with a recessed annular lip. As shown in Figure 26, under conventional injection strategies, spray/wall impingement occurs near the lip, and under the guidance of the combustion chamber wall, the spray is divided into two parts: the majority enters the bottom of the piston and forms a clockwise vortex core, while a minority develops upwards, crosses the step, enters the squish region, and forms a counterclockwise vortex core. Both vortex cores continue to grow over time and form large-scale vortex structures with strong air entrainment capabilities at the leading edge of the wall-attached fuel, especially structure A at the bottom of the piston. With increasing nozzle diameter, the scale and intensity of the vortices at the bottom of the piston increase, while the intensity of the vortices in the squish region decreases. This phenomenon is particularly evident 15 degrees after spray/wall impingement, as the larger nozzle diameter causes the spray/wall impingement point at the end of injection to be closer to the bottom of the piston, resulting in more fuel entering the piston and less fuel entering the squish region. Furthermore, the residual momentum of wall-attached fuel is relatively high, leading to larger scale and intensity of vortices at the bottom of the piston. Although increasing the nozzle diameter weakens the vortices in the squish region, comparing the oxygen concentration in the squish region under different nozzle diameters reveals that even with strong vortex structures in the squish region, it is difficult to entrain air between the piston and cylinder liner gaps. However, the strengthened vortices at the bottom of the piston can entrain a large amount of surrounding air into the vortex structure, facilitating the mixing of air and unburnt fuel within the vortex structure and improving the air utilization rate in the piston center region. Benefiting from the higher mixture quality inside the spray during the free development stage and the larger and stronger vortices induced after spray/wall impingement, the mixing of wall-attached fuel is enhanced, leading to an increase in the mixing quality after the spray/wall impingement stage.

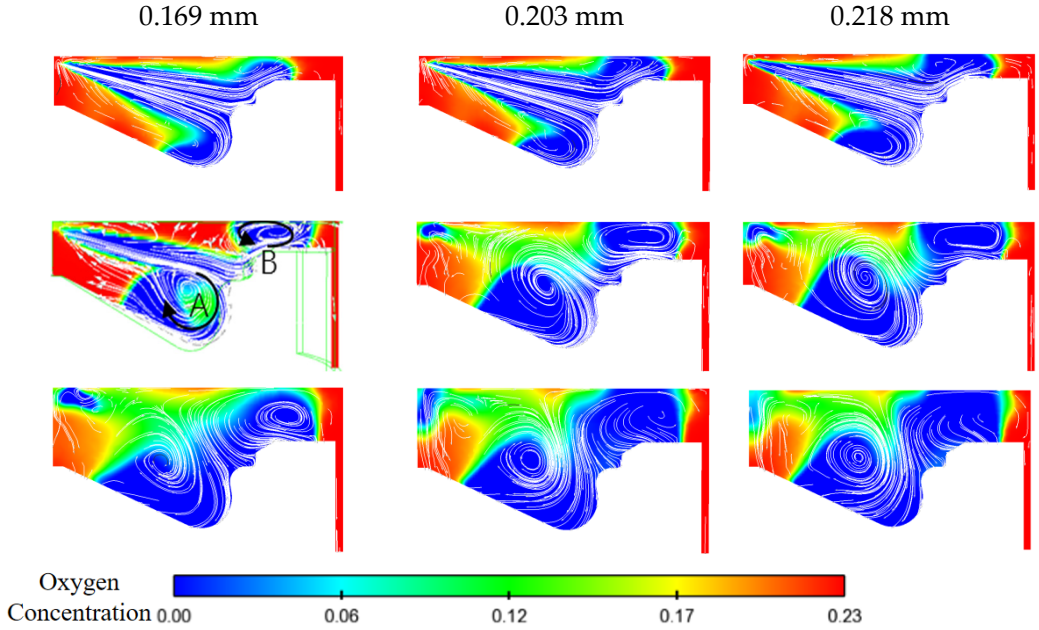

Figure 26. Distribution of in-cylinder flow field and oxygen concentration after spray/wall impingement for three nozzle diameters.

There are significant differences in the reaction pathways corresponding to different equivalence ratio ranges of the mixture, which inevitably lead to significant differences in the contribution to combustion heat release. Instantaneous heat release rates of mixture in different equivalence ratio ranges were statistically analyzed, as shown in Figure 27. When the nozzle diameter increases from 0.169 mm to 0.218 mm, due to the increase in the mass of fuel entering the cylinder per unit time, the heat release rates of mixture in different equivalence ratio ranges during the injector duration all show varying degrees

of improvement. The heat release contribution of lean mixtures with Φ < 1 is the highest, and the corresponding increase in heat release rate is most significant. This is also the key reason why increasing the nozzle diameter leads to the most significant increase in heat release rate.

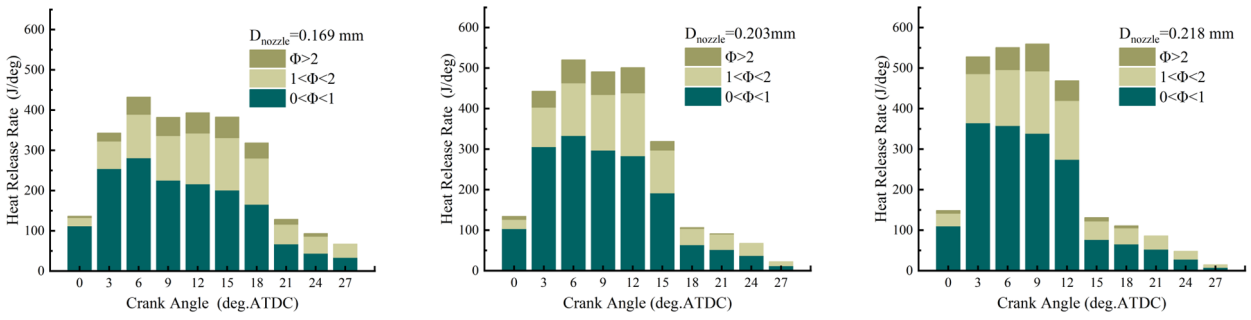

Figure 27. The instantaneous heat release rates of mixture in different equivalence ratio ranges for three injector nozzle diameters: (**a**) 0.169 mm; (**b**) 0.203 mm; (**c**) 0.218 mm.

In summary, the research results show that in a high charge density environment, increasing the nozzle diameter from 0.169 mm to 0.218 mm not only increases the mass of fuel entering the cylinder per unit time but also improves the overall mixture quality during the entire spray development process. The proportion of lean mixtures inside the spray increases, resulting in more combustible mixture being produced per unit time. As a result, the combustion heat release rate significantly increases, the combustion duration is notably shortened, and the proportion of constant volume combustion increases, allowing for more complete expansion of the working fluid, leading to an indicated thermal efficiency increase to 51.5%.

The above research was conducted within the range of experimental fuel injectors (0.169 mm to 0.218 mm). Given the limitations of the experimental fuel injector nozzle diameter range, numerical simulation methods were employed to expand the research scope of the fuel injector nozzle diameter in order to verify the applicability of the conclusions obtained within a wider range of nozzle diameters. Figure 28 shows the simulation results of the hydraulic system model of the fuel injector. With the increase in nozzle diameter, the actual fuel injection pressure shows a linear decreasing trend, the fuel injection rate continuously increases and the duration of fuel injection continuously shorten. However, when the nozzle diameter exceeds 0.2 mm, the rate of decrease in the duration of fuel injection significantly slows down. This means that the benefits of increasing the fuel injection rate decrease as the nozzle diameter increases, mainly because increasing the nozzle diameter will increases the pressure loss inside the fuel injector, resulting in an excessive decrease in the actual fuel injection pressure. In addition, expanding the research scope of the fuel injector nozzle diameter reveals that the spray momentum at the nozzle outlet per unit time shows a trend of initially increasing and then decreasing with increasing nozzle diameter. This is the result of the interplay between the nozzle flow area and the actual fuel injection pressure. Excessive enlargement of the nozzle diameter will lead to a significant decrease in spray momentum, thereby affecting subsequent droplet atomization, fuel–air mixture, and combustion processes. In this study, the nozzle diameter corresponding to the peak spray momentum at the nozzle outlet was within the range of 0.218 mm to 0.25 mm.

Figure 29 shows the numerical simulation results of the in-cylinder combustion process. When the nozzle diameter exceeds 0.25 mm, the decrease in spray momentum entering the cylinder per unit time leads to a reduction in the air entrainment rate, and the duration of free spray development is significantly shortened, resulting in deterioration of the mixture quality inside the spray at the spray/wall impingement moment. From the perspective of heat release rate, within the range of nozzle diameters from 0.13 mm to 0.25 mm, the combustion duration gradually shortens and the thermal efficiency significantly improves

as the nozzle diameter increases. Within the range of nozzle diameters from 0.25 mm to 0.37 mm, the combustion duration remains around 23 degrees and the thermal efficiency shows a slow decreasing trend as the nozzle diameter increases. Therefore, under the engine operating parameters and thermodynamic boundary conditions considered in this study, the optimal nozzle diameter should be within the range of 0.218 mm to 0.25 mm.

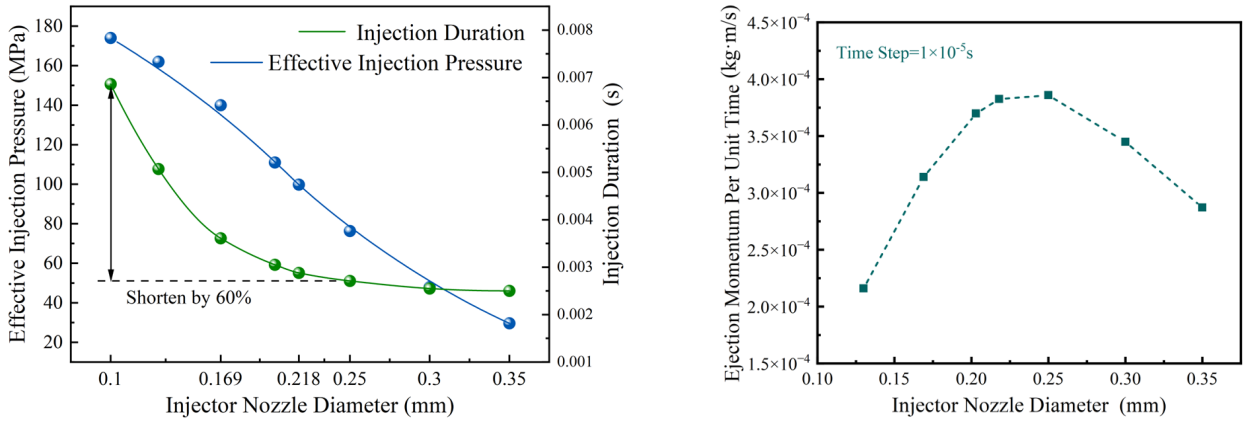

(**a**) (**b**)

Figure 28. Simulation results obtained from expanding the research scope of nozzle diameters: (**a**) effective injection pressure and fuel injection duration; (**b**) spray momentum at nozzle outlet.

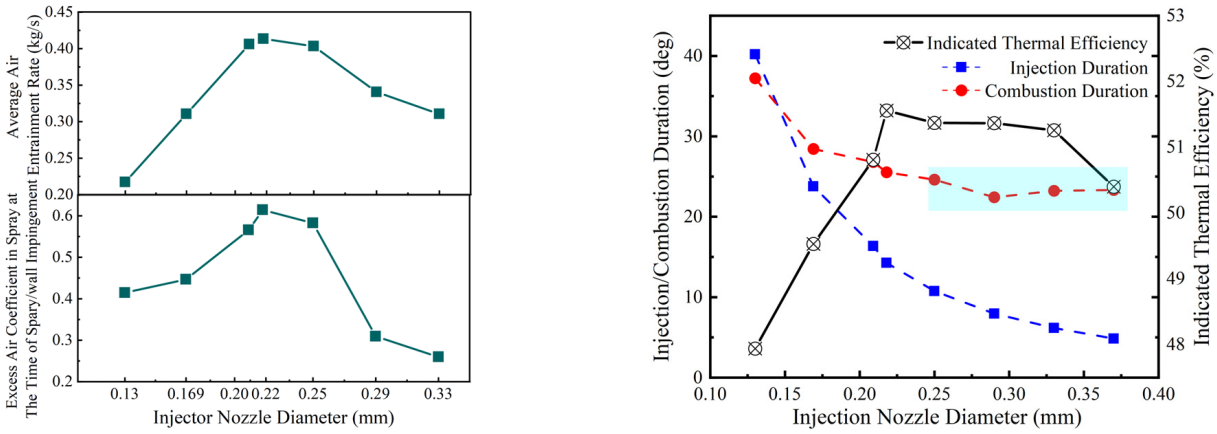

(**a**) (**b**)

Figure 29. Numerical simulation results obtained from expanding the fuel injector nozzle diameter range: (**a**) spray mixture quality; (**b**) combustion duration and indicated thermal efficiency.

5. Conclusions

In order to improve the fuel economy of heavy-duty diesel engines under high-load conditions, based on the combustion pathway model, it is proposed that the proportion of lean mixture with $0 < \Phi < 1$ is the most important spray characteristic affecting the overall diesel combustion process. Answering the question of how to increase the proportion of lean mixture inside the spray is the key to achieving efficient and clean combustion of diesel engines. Through experiment and numerical simulation methods, the following conclusions are drawn regarding the impact mechanism of fuel injector nozzle diameter on spray lean mixture characteristics, fuel–air mixture, and combustion process under high charge density conditions, as well as the potential to improve thermal efficiency:

In a high charge density environment, increasing the nozzle diameter from 0.169 mm to 0.218 mm can improve the overall mixture quality throughout the spray development process. The experimental results show that with the increase in nozzle diameter, the peak

pressure and instantaneous heat release rate significantly increase, the combustion duration is shortened by about 20%, the heat release becomes more concentrated, and the proportion of constant volume combustion increase. At 1200 rpm and IMEPg~2.3 MPa conditions, the indicated thermal efficiency increases by 1.3%, reaching a maximum of 51.5%.

With the increase in nozzle diameter, the spray ejection momentum per unit time also increases significantly. The increase in spray penetration velocity strengthens the friction and shear effects between the spray and fresh air, resulting in faster energy dissipation rates and a higher proportion of energy dissipation in the radial direction of the spray core, especially in the upstream region where the penetration velocity is highest. The higher spray momentum combined with the increased dissipation proportion means that larger nozzle diameter fuel injectors transfer more momentum to the fresh air radially, resulting in a wider radial distribution range of high-momentum regions in the middle region of the spray, intensifying the mass transfer and entrainment process at the spray edge.

Introducing the oxygen mass transport rate to evaluate the strength of air entrainment motion at various positions of the spray: during the free development process of the spray, oxygen forward transport is dominant; i.e., the oxygen transport rate parameter is greater than 0. During this process, a large amount of oxygen enters the interior of the spray, and the most intense oxygen transport occurs at the inner boundary of the gas phase spray with obvious oxygen concentration stratification. With the increase in nozzle diameter, the higher spray momentum during the free development stage leads to more intense oxygen transport motion, and the radial range of effective oxygen transport in the middle region of the spray increases significantly.

In the region near the spray outlet where liquid-phase fuel evaporation is dominant, high air entrainment leads to a significant increase in the amount of gas-phase fuel generated, which is beneficial for subsequent fuel–air mixing. The proportion of rich mixture increases rapidly, the mass fraction of lean mixture inside the spray reaches its peak until the spray/wall impingement moment. Increasing the nozzle diameter increases the air entrainment by 42% during the free development stage of the spray, and the proportion of lean mixture inside the spray increases from 60.2% to 64.0%. Benefit from the higher mixture quality during the free development stage of the spray and the larger and stronger vortex generated at the front of the spray after spray/wall impingement, increasing the nozzle diameter intensifies the mixing process between the wall-attached fuel and air, leading to an improvement in the mixture quality after the spray/wall impingement stage. Overall, increasing the nozzle diameter from 0.169 mm to 0.218 mm increases the mass of fuel entering the cylinder per unit time, while also increasing the proportion of lean mixture throughout the entire spray development process, resulting in an increase in the heat release rate of the lean mixture, making the overall combustion more intense and concentrated.

By using numerical simulation methods to expand the research scope of fuel injector nozzle diameters, the applicability of the conclusions obtained within a wider range of nozzle diameters is verified. It is found that a nozzle diameter that is too small sacrifices fuel injection duration, leading to a large amount of fuel combustion during the piston descent process, while a nozzle diameter that is too large leads to an excessive reduction in effective injection pressure, affecting spray momentum and subsequent fuel–air mixture processes, with no further reduction in combustion duration but a slow decrease in thermal efficiency. Under the engine operating parameters and thermodynamic boundary conditions considered in this study, the optimal nozzle diameter should be in the range of 0.218 mm to 0.25 mm.

Author Contributions: Conceptualization, W.S. and Y.L.; methodology, Y.L.; software, Y.L.; validation, Y.L.; formal analysis, Y.L.; data curation, Y.L.; writing—original draft preparation, Y.L.; writing—review and editing, W.S.; funding acquisition, W.S. All authors have read and agreed to the published version of the manuscript.

Funding: This research was funded by the National Key Research and Development Program of China (No. 2022YFE0100100).

Data Availability Statement: The data presented in this study are available on request from the corresponding author. The data are not publicly available due to privacy.

Conflicts of Interest: The authors declare no conflicts of interest.

Nomenclature

Item	Definition
NOx	Nitrogen Oxide
UHC	Unburnt Hydrocarbon
ATDC	After Top Dead Center
CA	Crank Angle
ECU	Electronic Control Unit
EGR	Exhaust Gas Recirculation
Φ	Fuel–oxygen Equivalence Ratio
CA10	10% Heat Release Point
Ca50	50% Heat Release Point
Ca90	90% Heat Release Point
HRR	Heat Release Rate
IMEP	Indicated Mean Effective Pressure
ITEg	Gross Indicated Thermal Efficiency

References

1. Huang, M.; Zhai, P. Achieving Paris Agreement temperature goals requires carbon neutrality by middle century with far-reaching transitions in the whole society. *Adv. Clim. Chang. Res.* **2021**, *12*, 281–286. [CrossRef]
2. Gunfaus, M.T.; Waisman, H. Assessing the adequacy of the global response to the Paris Agreement: Toward a full appraisal of climate ambition and action. *Earth Syst. Gov.* **2021**, *8*, 100102. [CrossRef]
3. Senecal, P.; Leach, F. Diversity in transportation: Why a mix of propulsion technologies is the way forward for the future fleet. *Results Eng.* **2019**, *4*, 100060. [CrossRef]
4. Kumano, K.; Iida, N. Analysis of the effect of charge inhomogeneity on HCCI combustion by chemiluminescence measurement. *J. Fuels Lubr.* **2004**, *113*, 974–986.
5. Verma, S.K.; Gaur, S.; Akram, T.; Gautam, S.; Kumar, A. Emissions from homogeneous charge compression ignition (HCCI) engine using different fuels: A review. *Green Energy Environ. Sustain.* **2022**, *29*, 50960–50969. [CrossRef] [PubMed]
6. Liu, Y.; Su, W.; Wu, B.; Wang, J. The Research and Development of a Jet Disturbance Combustion System for Heavy-Duty Diesel Engines. *Energies* **2024**, *17*, 1065. [CrossRef]
7. Zhang, Z.; Liu, Y.; Wu, B.; Nie, J.; Su, W. Effect of Nozzle Diameter on Combustion and Emissions of a Heavy Duty Diesel Engine. *Trans. CSICE* **2022**, *40*, 97–105.
8. Zhai, C.; Jin, Y.; Nishida, K.; Ogata, Y. Diesel spray and combustion of multi-hole injectors with micro-hole under ultra-high injection pressure–non-evaporating spray characteristics. *Fuel* **2021**, *283*, 119322. [CrossRef]
9. Zhao, J.; Grekhov, L.; Yue, P. Limit of fuel injection rate in the common rail system under ultra-high pressures. *Int. J. Automot. Technol.* **2020**, *21*, 649–656. [CrossRef]
10. Wang, L.; Lowrie, J.; Ngaile, G.; Fang, T. High injection pressure diesel sprays from a piezoelectric fuel injector. *Appl. Therm. Eng.* **2019**, *152*, 807–824. [CrossRef]
11. Shi, Z.; Wu, H.; Li, H.; Zhang, L.; Lee, C. Effect of injection pressure and fuel mass on wall-impinging ignition and combustion characteristics of heavy-duty diesel engine at low temperatures. *Fuel* **2021**, *299*, 120904. [CrossRef]
12. Xia, J.; Zhang, Q.; Huang, Z.; Ju, D.; Lu, X. Experimental study of injection characteristics under diesel's sub/trans/supercritical conditions with various nozzle diameters and injection pressures. *Energy Convers. Manag.* **2020**, *215*, 112949. [CrossRef]
13. Dec, J. *A Conceptual Model of DI Diesel Combustion Based on Laser-Sheet Imaging*; SAE Technical Paper 970873; JSTOR: New York, NY, USA, 1997.
14. Pickett, L.M.; Siebers, D.L. Non-sooting, low flame temperature mixing-controlled DI diesel combustion. *SAE Trans.* **2004**, *113*, 614–630.
15. Kook, S.; Bae, C.; Miles, P.C.; Choi, D.; Pickett, L.M. The influence of charge dilution and injection timing on low-temperature diesel combustion and emissions. *SAE Trans.* **2005**, *114*, 1575–1595.
16. Polonowski, C.J.; Mueller, C.J.; Gehrke, C.R.; Bazyn, T.; Martin, G.C.; Lillo, P.M. An experimental investigation of low-soot and soot-free combustion strategies in a heavy-duty, single-cylinder, direct-injection, optical diesel engine. *SAE Int. J. Fuels Lubr.* **2012**, *5*, 51–77. [CrossRef]

17. Manin, J.; Skeen, S.; Pickett, L.M.; Kurtz, E.; Anderson, J.E. Effects of oxygenated fuels on combustion and soot formation/oxidation processes. *SAE Int. J. Fuels Lubr.* **2014**, *7*, 704–717. [CrossRef]
18. Dumitrescu, C.E.; Mueller, C.J.; Kurtz, E. Investigation of a tripropylene-glycol monomethyl ether and diesel blend for soot-free combustion in an optical direct-injection diesel engine. *Appl. Therm. Eng.* **2016**, *101*, 639–646. [CrossRef]
19. Huang, H. Numerical and Experimental Study on the Combustion Process of Diesel HCCI Engines. Ph.D. Dissertation, Tianjin University, Tianjin, China, 2007.
20. Wang, H.; Zheng, D.; Tian, Y. High pressure common rail injection system modeling and control. *ISA Trans.* **2016**, *63*, 265–273. [CrossRef] [PubMed]
21. Kim, J.; Lee, J.; Kim, K. Numerical study on the effects of fuel viscosity and density on the injection rate performance of a solenoid diesel injector based on AMESim. *Fuel* **2019**, *256*, 115912. [CrossRef]
22. Blessing, M.; König, G.; Krüger, C.; Michels, U.; Schwarz, V. Analysis of flow and cavitation phenomena in diesel injection nozzles and its effects on spray and mixture formation. *SAE Trans.* **2003**, *112*, 1694–1706.
23. Zhang, X. Research on Interaction of Physical and Chemical Factors in MULIN-BUMP Compound Combustion. Ph.D. Dissertation, Tianjin University, Tianjin, China, 2007.